Environmental Science & Technology

Article

pubs.acs.org/est

Biomimetic Hydrogel Composites for Soil Stabilization and Contaminant Mitigation

Zhi Zhao,[†,‡] Nasser Hamdan,[‡] Li Shen,[†] Hanqing Nan,[†] Abdullah Almajed,[‡] Edward Kavazanjian,[‡] and Ximin He*[,†,‡,§]

[†]School for Engineering of Matter, Transport and Energy, Arizona State University, 781 E Terrace Rd, Tempe, Arizona 85287, United States

[‡]The Center for Bio-inspired and Bio-mediated Geotechnics, Arizona State University, P.O. Box 873005, Tempe, Arizona 85287-3005, United States

[§]The Biodesign Institute, Molecular Design and Biomimetics Center, Arizona State University, 727 E. Tyler St., Tempe, Arizona 85287-5001, United States

Supporting Information

ABSTRACT: We have developed a novel method to synthesize a hyper-branched biomimetic hydrogel network across a soil matrix to improve the mechanical strength of the loose soil and simultaneously mitigate potential contamination due to excessive ammonium. This method successfully yielded a hierarchical structure that possesses the water retention, ion absorption, and soil aggregation capabilities of plant root systems in a chemically controllable manner. Inspired by the robust organic−inorganic composites found in many living organisms, we have combined this hydrogel network with a calcite biomineralization process to stabilize soil. Our experiments demonstrate that poly(acrylic acid) (PAA) can work synergistically with enzyme-induced carbonate precipitation (EICP) to render a versatile, high-performance soil stabilization method. PAA-enhanced EICP provides multiple benefits including lengthening of water supply time, localization of cementation reactions, reduction of harmful byproduct ammonium, and achievement of ultrahigh soil strength. Soil crusts we have obtained can sustain up to 4.8 × 10^3 kPa pressure, a level comparable to cementitious materials. An ammonium removal rate of 96% has also been achieved. These results demonstrate the potential for hydrogel-assisted EICP to provide effective soil improvement and ammonium mitigation for wind erosion control and other applications.

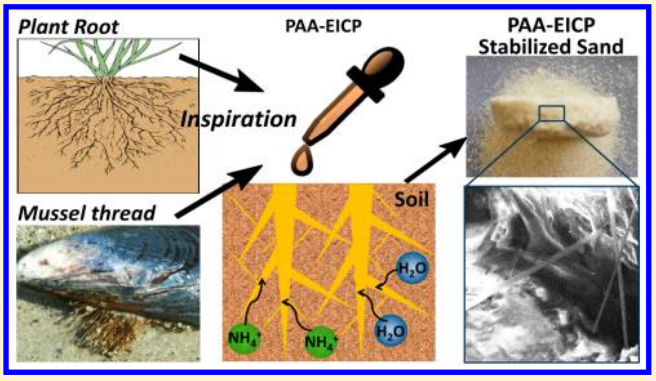

INTRODUCTION

Environmental degradation, especially soil instabilities that arise from cohesionless and polluted soil, has become an increasingly important global issue.[1] For example, fugitive dust emission[2] has caused extensive negative impacts on human health and safety.[3] Effectively aggregating loose cohesionless granular soils to improve their inherent poor mechanical strength is crucial to solving the pressing issues of wind or water erosion of earth surface,[4] earthquake-induced liquefaction,[5] and many instability-induced troubles in constructional projects.[6,7] In addition, anthropogenic activities may discharge various pollutants to the environment, among which ammonium (NH_4^+) is a major issue.[8−10] Excessive NH_4^+ can cause eutrophication in watercourses,[11,12] lead to higher levels of toxic nitrogen-containing compounds,[13] elevate greenhouse gases generation,[14] and accelerate soil acidification. Interestingly, a significant portion of NH_4^+ in aqueous systems comes from the leachate of loose, highly permeable soils.[9] As a result, efficient soil stabilization solutions that can simultaneously fulfill the need for effectively aggregating loose soil, increasing the mechanical strength of soil, and mitigating soil pollutants have significant value.

Traditional soil stabilization methods usually involve heavy machinery and energy intensive processes that result in CO_2 emissions, excessive consumption of natural resources, and generation of hazardous waste.[15,16] Some recently developed methods based on using organic or inorganic soil stabilizers are less energy consuming, but still have various disadvantages.[17−20] As organic stabilizers, natural polymers are usually biodegradable, which limits the lifetime of their stabilization effect.[21] Common inorganic stabilizers such as salts offer limited short-term soil stabilization that is easily reversed by rain or possibly atmospheric moisture, in addition to their significant negative impacts on soil quality, groundwater,

Received: March 15, 2016
Revised: August 29, 2016
Accepted: October 20, 2016
Published: October 20, 2016

DOI: 10.1021/acs.est.6b01285
Environ. Sci. Technol. 2016, 50, 12401−12410

vegetation, and roadway environments.[22−24] Furthermore, soil stabilizers are rarely able to reach a soil strength level comparable to cement-treated samples, nor are they capable of mitigating soil pollutants.

Nature can provide great inspiration on how to overcome the challenges in soil stabilization. Many living organisms use a combination of inorganic and organic compounds to build stable and robust materials. For example, mussel byssal threads employ Fe^{3+} stabilized proteinaceous glue filaments to help them withstand large cyclic strains.[25] Strong biomaterials such as bones and seashells use occlusion of macromolecules within individual crystals to generate superior mechanical properties.[26] Despite the wide presence and great benefits of this biochemical pathway in nature, a similarly strategy is rarely employed in soil stabilization or remediation due to the difficulties in integrating organic and inorganic compounds into a composite in soil. Enzyme induced carbonate precipitation (EICP)[27−29] provides a controllable way to introduce inorganic crystals within soil to address concerns regarding environmental degradation[27,28,30,31] and provide suitable ground for civil infrastructure construction.[32] Hydrogel is a promising organic candidate for soil stabilization.[33−37] Compared with naturally occurring polymers,[38] synthetic hydrogels are more controllable and flexible in their molecular structures and compositions, which makes it possible to chemically engineer synthetic hydrogels to render a soil stabilizer that consists of inorganic−organic composites by combining hydrogels and EICP.

To design a hydrogel-EICP composite with effective structural and chemical functions, we borrowed our strategy from plants that have developed an extensive network of roots to tightly anchor themselves in the soil.[39] The hyper-branched root system of plants are known to facilitate aggregation of soil particles.[40,41] Structurally mimicking the unique root structure with hydrogel material can provide additional enhancement to soil in terms of higher strength and a larger length scale of continuity. In addition, root systems feature high water affinity and great ion absorbing ability in order to constantly provide their stems and leaves with water and dissolved minerals.[41,42] Realizing these properties in a chemical manner is preferred for retaining water, localizing inorganic reagents to improve the yield in biomineralization, and enhancing the mechanical strength of the hydrogel-EICP composite through cation-hydrogel complexation.[25] Additionally, the removal of ammonium, a byproduct in EICP, may also be achieved through mimicking the ion absorbing ability of roots with proper functional groups in the hydrogel.[43−45]

Herein, we present an innovative method to locally synthesize a poly(acrylic acid) (PAA) hydrogel network with minerals coprecipitated via the EICP process in the soil matrix to form an organic−inorganic composite soil stabilizer which mimics plant root systems. It is worthwhile to note that acrylic acid is known for its nontoxicity to soil/water living organisms.[46] The injectable precursor solution we developed can (1) be cured in situ in soil over controllable time and form root-like structures, (2) facilitate the carbonate precipitating of EICP into composites to form a uniform gel-calcite-soil network, and (3) result in remarkable surface soil stabilization performance with significantly enhanced mechanical strength of soil and contaminant mitigation, exhibiting similar functions to a plant root system. The synthetic method has been carefully investigated. Various characterizations, including SEM, EDX, XRD, vapor pressure measurement, and strength test, were conducted to examine the product. Ammonium absorption/desorption was also investigated through spectral measurements. The overall performance of the PAA-EICP composite as a soil stabilizer was compared with the effectiveness of a conventional EICP solution to illustrate the advantages of our method.

MATERIALS AND METHODS

Chemicals. Hydrochloric acid (ACS grade), sodium hydroxide (≥98%), phosphoric acid (ACS grade), acrylic acid (AA, 99%), *N*,*N*′-methylenebis(acrylamide) (Bis, 99%), 2-hydroxy-4′-(2-hydroxyethoxy)-2-methylpropiophenone (Igarcure 2959, 98%), ammonium persulfate (APS, 98%), sodium hydroxide (≥98%), ammonium chloride (≥99.5%) and urease (15 000−50 000 units/g) from *Canavalia ensiformis* (Jack bean) were purchased from Sigma-Aldrich. Calcium chloride dihydrate (ACS grade) and sodium phosphate, dibasic (≥98%) were purchased from G-Biosciences. Nessler's reagent was purchased from Fluka.

Hydrogel Preparation. Cross-linked polyacrylate gel (x-PAA) was prepared by dissolving 400 mg acrylic acid, 20 mg Bis and 10 mg Igarcure 2959 in 1 mL DI water (Elga Ultra Analytic Lab Water Purification System). The mixture was then cured under UV light (Dymax 5000-EC UV light curing flood system) for 30 s.

Cementation Localization Test. A thermally curable PAA precursor (t-AA) that could be directly injected into soil was developed. The recipe for this precursor can be found in the Supporting Information. A cementation localization test was conducted using centrifuge tubes filled with fine-grained silica sand (F-60 silica sand, typical engineering sand used in soil stabilization studies). The EICP solution was prepared by mixing a $CaCl_2$-urea solution with a urease solution in a 4:1 volume ratio. The final concentrations of reactants in EICP solution were: 1.000 M $CaCl_2{\cdot}(2H_2O)$, 1.500 M urea and 0.450 mg/mL urease. t-AA of various volume fractions (0, 20, 40, 50, 60, 80, and 100%) were mixed with the EICP solution and the mixture was poured onto soil surface immediately after mixing at a dose of 3 mL/in^2. Control samples treated with a solution that did not contain enzyme were also prepared with the same method. All the centrifuge tubes were kept at 40 °C (Fisher Scientific Isotemp Premium Lab Oven) for 5 h followed by incubating at room temperature (RT) for 14 days to allow time for the cementation reaction to take place.

Characterization Methods. All the SEM and EDX data was taken using a 15 keV Hitachi S4700 field emission scanning electron microscope. Powder XRD data on the carbonate crystals formed in PAA-enhanced EICP was recorded using a Siemens D5000 X-ray powder diffraction system. The unconfined compressive strength of soils stabilized by PAA containing solutions was measured by a uniaxial compression machine (GCTS STX-050 pneumatic cyclic triaxial system). Fourier transform infrared (FTIR) spectra were measured by an IFS 66v/S vacuum FT-IR (Bruker Optics) in the attenuated total reflection (ATR) mode. X-ray photoelectron spectroscopy (XPS) spectra were measured with a VG 220i-XL X-ray photoelectron spectrometer. Samples were dried in a vacuum oven at 50 °C overnight to remove physically absorbed water before FTIR and XPS measurements. An accelerated weathering test was carried out in an environmental chamber (QUV Accelerated Weathering Tester). Detailed experimental procedures are included in the Supporting Information.

DOI: 10.1021/acs.est.6b01285
Environ. Sci. Technol. 2016, 50, 12401−12410

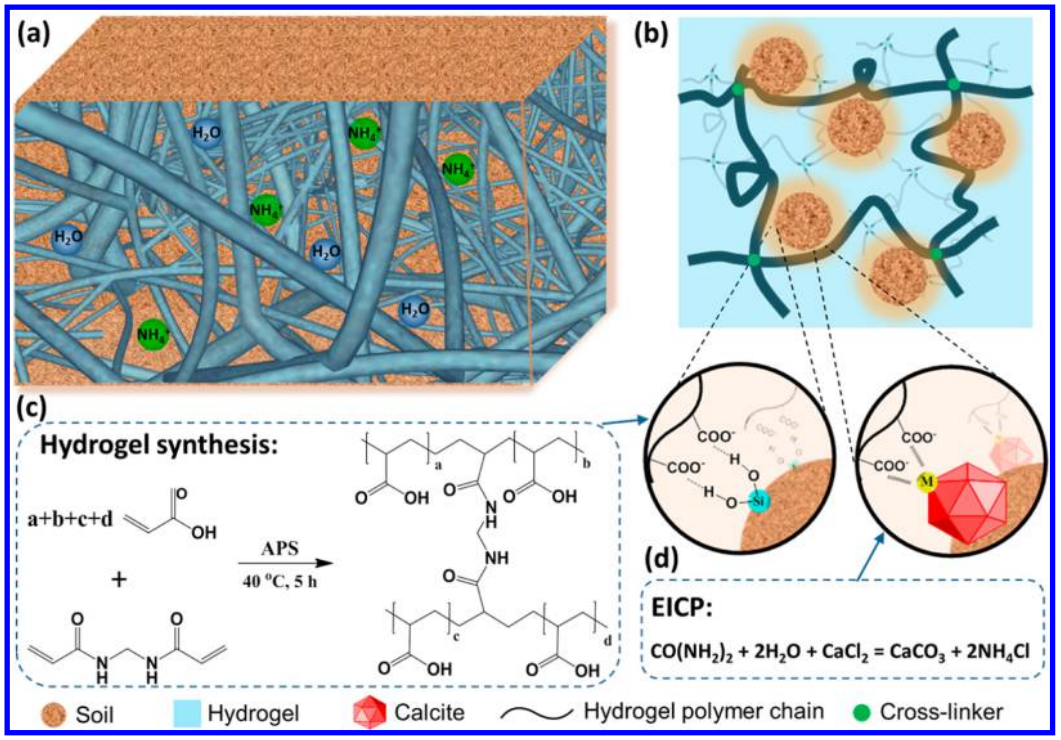

Figure 1. (a) A conceptual image of the hyper-branched hydrogel network formed in soil matrix that resembles plant roots, providing good water retention and contaminant (NH_4^+) mitigation functions in soil stabilization; (b) A scheme showing the expected interactions between the hydrogel and soil particles or the calcite crystals from ECIP. Inset: zoomed in image of the hydrogel bonding (left) and complexation interactions (right); (c) The reaction formula of hydrogel synthesis; (d) The reaction formula of EICP.

RESULTS AND DISCUSSION

The Biomimetic PAA Network. In-situ synthesis of a root-like hydrogel network in the soil is the key step in this novel biomimicry approach for soil stabilization (Figure 1). Figure 1a shows a conceptive image of the hydrogel structure consisting of a major network and a secondary network featuring a higher degree of cross-linking, resembling the taproot and subsidiary roots of natural plants, respectively. The functional groups on the hydrogel structure will allow it to efficiently interact with soil particles, minerals (calcite, etc.) and free ions (NH_4^+, *etc.*) (Figure 1a and b). SEM images in Figure 2 of F-60 sand treated with t-AA and ECIP reagents showed that a hierarchical, hyper-branched hydrogel structure successfully formed in sand through in situ polymerization. A number of filaments of a few microns in diameter and hundreds of micron in length were found to exist between sand particles (Figure 2a,b and Figure S1a). EDX confirmed that the filaments were rich in carbon, which indicated its polymeric nature (Figure S1b). Those hydrogel filaments directly grew from amorphous polymer layers (Figure 2a, inset) and connected multiple well-separated sand particles. Specifically, the hydrogel filaments attached to different sand particles can form covalent connections, leading to branched structures that bridge the sand particles and thus stabilize the matrix (red dashed lines in Figure 2b). Multivalent connections between sand particles and individual filaments are also found to exist (Figure 2c). It is expected that sand particles far away from each other could be fixed by such a "scaffold". Each individual particle may have many filaments attached, leading to a major network similar to the well spreading taproot (Figure S1c). Meanwhile, a porous hydrogel structure is observed to cover most surfaces of individual sand particles and effectively filled the interparticle spaces between adjacent sand particles, well resembling the localized subsidiary roots (Figure 2d). The porous structure showed a highly cross-linked appearance with an average pore size of ~2 μm (Figure 2e). It is worthwhile to note that the porous structure was interconnected by hydrogel filaments and their joint points were revealed by SEM (Figure 2d, red arrows), which suggests that the two different hydrogel structures can be expected to work as a unified system. To the best of our knowledge, this is the first time that such unique features have been demonstrated in soil stabilization. Such a hierarchical network is believed to make a significant contribution to the superior stabilization performance of this method.

The filament-connected porous polymer network that we obtained herein is a distinct characteristic of synthetic hydrogels. Our previous work[38] demonstrated that biopolymers (normally non-cross-linked) only formed amorphous structures with a much smoother appearance (Figure S1d). The long filaments we observed in this work were postulated to form via metal ion mediated assembly of polymer chains, as previous research showed that organic ligands, such as carboxyl groups existing in PAA, could form complexes with various cations existing in the EICP solution and sand system, including NH_4^+, Mg^{2+}, and Ca^{2+} through complexation or electrostatic interactions.[47] In our reaction system, the concentration of metal cations was at the level of moles per liter, sufficient to affect the polymer assembling. Details of the mechanism will be pursued in our future work.

Our experiment indicated that there appeared to be no interference between hydrogel polymerization and EICP. As can be seen in Figure 2f, clusters of mineral crystals grew within hydrogel networks when F-60 soil samples were treated with a mixture of t-AA and EICP solution. EDX and XRD characterizations have confirmed that the major form of those

DOI: 10.1021/acs.est.6b01285
Environ. Sci. Technol. 2016, 50, 12401−12410

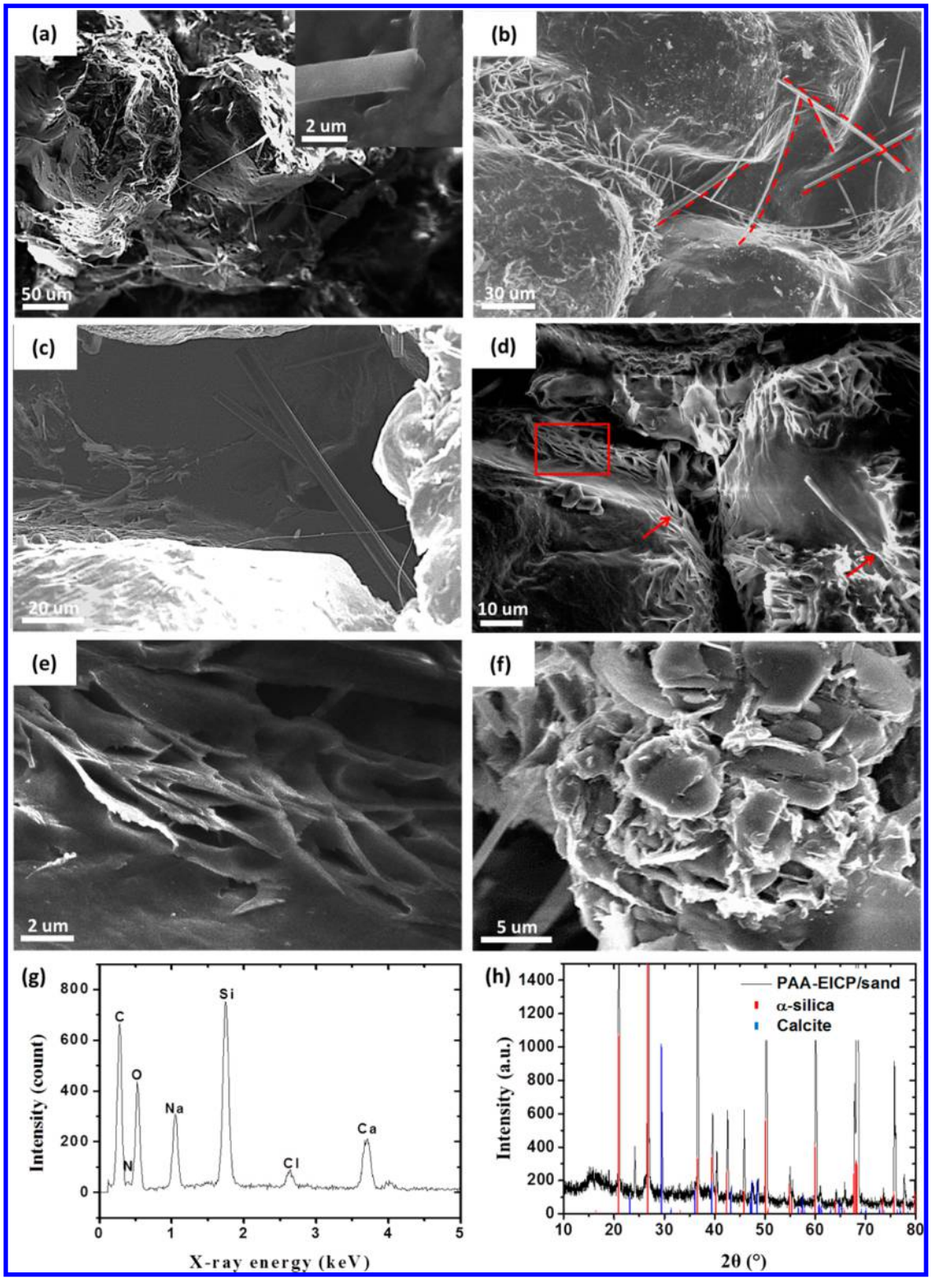

Figure 2. Various characterizations of sand samples treated with PAA-EICP stabilizer solution. (a) Long polymer filaments connecting sand particles. Inset: a zoom-in image of the joint point between the filament and bulk hydrogel; (b) Interconnected PAA filaments between sand particles; (c) A zoom-in image of a branched filament that spans the interparticle gap; (d) Porous hydrogel structure on and between sand particles. Red arrows point to the joint points between porous hydrogel structure and PAA filaments; (e) Magnified image of the red rectangular region in (d); (f) SEM image of a PAA-calcite composite; (g) EDX spectrum of the same area in (f); (h) Powder XRD spectrum for sand samples stabilized by PAA and EICP.

crystals was calcite (Figure 2g and h). The elemental composition in the composite was 58.07% C, 7.33% N, 21.32% O, 3.67% Na, 6.09% Si, 0.66% Cl, and 2.66% Ca. Some tiny mismatches between experimental XRD peaks and reference peaks were presumably due to the presence of amorphous hydrogel in the intercrystal spaces. With its unique

DOI: 10.1021/acs.est.6b01285
Environ. Sci. Technol. 2016, 50, 12401−12410

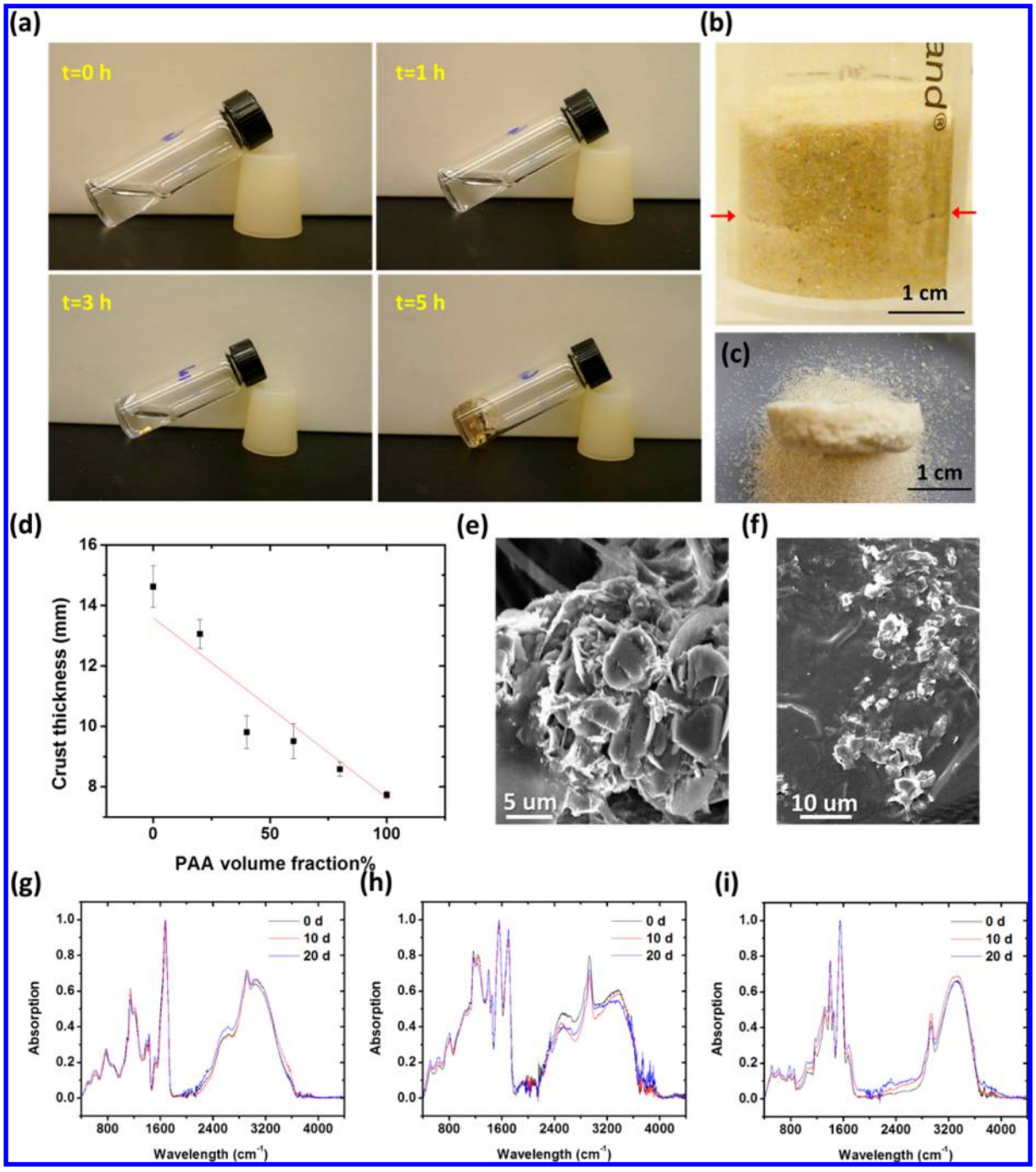

Figure 3. (a) Time lapse images of the spontaneous curing of a PAA precursor; (b) A representative image of the formation of a soil crust, well localized on the top surface of the soil in a tube. The red arrows point to the color difference and minor cracks, indicating the boundary between the localized precipitate region and the unbound sand; (c) Side view of soil crust taken out of the tube in (b) after removing unbound sand particles; (d) The relationship between the t-AA volume fraction in soil stabilizer and its penetration depth; Representative SEM image of the calcite crystals obtained under (e) 60% t-AA and (f) 20% t-AA; (g)-(i) FTIR spectra of PAA hydrogels before and after aging in the environmental chamber with (g) pristine carboxyl groups, (h) partially deprotonated carboxyl groups, and (i) carboxylate groups.

structure and chemical composition, the "artificial root" system developed herein is expected to work in a similar manner to a plant roots to realize the following functions in soil stabilization. First, the physical enwrapping of soil particles with polymer filaments and the porous polymer structure, as well as the chemical interactions between soil particles and the hierarchical network (e.g., van der Waals force, hydrogen bonding), should help soil aggregates form and sustain external stresses. Second, the porous hydrogel structure containing carboxyl groups should favor water/reactant retention and ion absorption, which resembles the biological functions of plant roots.

Water Retention by PAA Hydrogel. Since water is a necessary reactant in EICP, it is expected that employing hydrophilic PAA molecules will help retain water longer in the reaction system and reduce water loss due to evaporation and permeation so as to facilitate calcite precipitation. We have observed that it required a longer time (~14 days) for the PAA-

DOI: 10.1021/acs.est.6b01285
Environ. Sci. Technol. 2016, 50, 12401−12410

EICP solution to completely dry compared with pure EICP solutions.[48] Vapor pressure[49−51] measurement showed that adding PAA into DI water could significantly lower the evaporation rate (Figure S2a). The interactions between PAA and water molecules were energetically favorable, which was attributed to the carboxyl rich, super hydrophilic structure of PAA (Figure S2b). Although the tests were based on un-cross-linked PAA, the results may also be applied to cross-linked hydrogels (e.g., x-PAA). It has been shown that cross-linked polymers are better able to hold water because of the confinement effect induced by polymer networks.[52] Therefore, we expect x-PAA will provide even better water retention than PAA.

Localization of the Biomineralization Reactions. To ensure the successful in situ formation of an "artificial root" system, and for the convenience of future field applications, the following criteria needed to be met by the thermal-curable hydrogel precursor: (1) a sufficient polymerization reaction rate at ambient conditions; and (2) appropriate diffusion and permeation behavior to allow for filling up of the interparticle spaces in the soil. To fulfill these goals, the optimal concentration of APS and Bis was obtained through a series of experiments based on commonly known polymerization kinetics.[53] With this optimal concentration, the t-AA precursor spontaneously got cured within 5 h at 40 °C (Figure 3a). This temperature is commonly seen at surficial soils in arid and semiarid climates where fugitive dust is a major problem. When a different environmental temperature exists, the recipe can be tuned accordingly in a similar manner to obtain a desirable curing speed. During the gravity-driven permeation of a t-AA solution into soil, the thermal initiator would gradually initiate the polymerization, leading to increasing viscosity that slowed down the diffusion of t-AA. The entire precursor was able to diffuse in soil in about ∼3 h, which was slightly shorter than the gelation time of plain hydrogel (well controlled at 4−5 h). This small difference in time allowed the entire precursor to enter soil while prevented it from overpenetrating into deep regions within the ground. After t-AA containing EICP solution was applied onto the soil surface, the odor of NH_3 was detected in the headspace, indicating that urea hydrolysis was occurring. The reaction mixture was observed to be restricted within the upper layer of soil, indicating that hydrogel can effectively facilitate the retention of the reactants at the targeted location. A surficial soil crust was formed in all tubes where the reaction mixture was added (Figure 3b and c).

The addition of t-AA limited solution penetration to less than 13 mm while pure EICP reagent penetrated deeper (>14 mm) into the soil. The viscosity of the EICP-hydrogel solution was proportional to the volume fraction of t-AA. To further illustrate that the localization of the EICP solution was determined by solution viscosity, mixtures of different EICP:t-AA volume ratios were tested. It was found that the soil crusts formed with high t-AA volume fractions were generally thinner and more well-defined than crusts that formed using low t-AA volume fractions, demonstrating that the localization of EICP in the upper layer of soil was primarily due to the effect of t-AA solutions' viscosity on penetration. The relationship between t-AA volume fraction and crust thickness is shown in Figure 3d. These results clearly showed that the water-laden matrix formed by the EICP-hydrogel solution focused the $CaCO_3$ precipitation near the soil surface via a temporary reduction in the soils' hydraulic transmissivity, which should improve EICP efficiency. Furthermore, the increased viscosity temporarily slowed the off gassing of CO_2 and NH_3, further enhancing the EICP process. SEM images reveal that large clusters of calcite crystals, enwrapped by PAA networks, are formed at 50−60% t-AA volume ratios, clearly indicating the remarkable enhancement of EICP by using PAA (Figure 3e). Under those conditions, a decent viscosity could be reached with relatively high t-AA volume ratios while the calcium/urea concentrations were still sufficient to support the crystallization process. In comparison, only individual small calcite crystals were formed at higher EICP volume ratios, presumably due to the lack of physical confinement of the reactants (Figure 3f).

Mechanical Properties of Soils Fixed by PAA-EICP Mixture. Mechanical property tests was first conducted using the fall cone apparatus, an index test commonly used to establish the shear strength of cohesive soil specimens,[54] to demonstrate the significant enhancement of soil strength (Supporting Information, Section 3). It was shown that as the t-AA volume fraction increased, the soil crust became stronger. The fall cone showed that for a volume ratio of t-AA ≥ 40%, no penetration was observed even with the most aggressive cone (Table S2). Unconfined compressive strength of the soil samples was further measured by a compression machine. It was found that the hardest soil crust, stabilized with PAA was able to withstand contact pressures of 4.8×10^3 kPa (Figure S3a). A short video clip has been included in the Supporting Information to visually demonstrate the hardness of the treated soil samples. In comparison, untreated sand had almost no pressure resistance, while EICP-only treated soil was only able to resist as much as 64 kPa pressure (Figure S3b). The ultrahigh strength achieved using hydrogel assisted EICP was comparable to cement materials and has never been seen in previous EICP or hydrogel-assisted EICP experiments.[38,48] We attribute such extraordinary strength enhancement to the continuous, root-like network structure of PAA. At a molecular level, polymer chains in the hydrogel were held together through strong covalent bonds (instead of the weak Van der Waal force in synthetic non-cross-linked polymers and biopolymers), resulting in a highly stable polymeric structure. Microscopically, the hierarchical network helped to retain soil aggregations when displacement of various length scales occurred between soil particles.

Stability of PAA Hydrogel Network under Environmental Conditions. It is important that PAA networks remain mostly intact during the period of desired application under real environmental conditions. UV and thermal degradations commonly occur at soil surfaces where soil stabilizers are exposed to sunlight.[55] To evaluate the influence of UV irradiation and heat on PAA stabilities, an accelerated weathering test has been carried out. PAA hydrogels with pristine carboxyl groups, partially deprotonated carboxyl groups and carboxylate groups were tested to evaluate the potential effect of pH on PAA stability. The aged samples were first characterized with FTIR to examine changes in molecular structures. Under all test conditions, no obvious changes were observed in either the peak positions or the relative intensities during the test period (Figure 3g−i), indicating that PAA remained intact. In addition, pH did not seem to affect the short-term stability of PAA. The result was consistent with previously reported findings. It has been previously shown that PAA is thermally stable under moderate temperatures.[56,57] The initial decomposition involving the formation of anhydrides was not likely to happen until the temperature reached ∼150 °C.

DOI: 10.1021/acs.est.6b01285
Environ. Sci. Technol. 2016, 50, 12401−12410

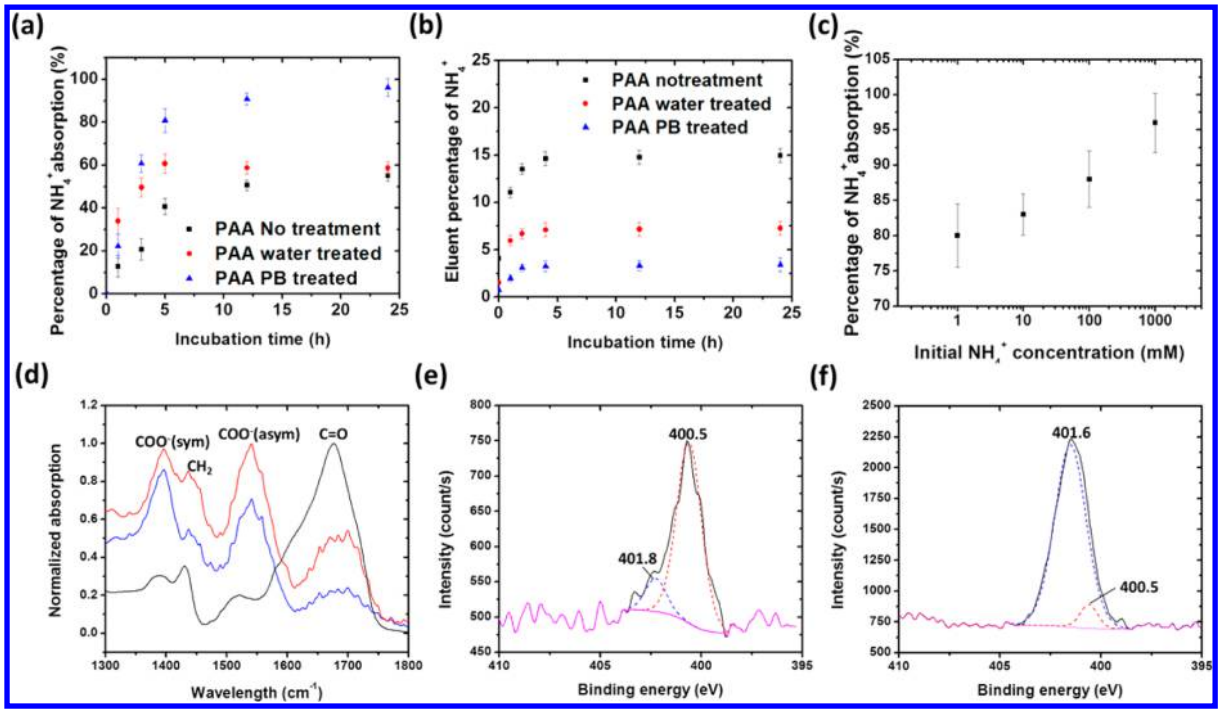

Figure 4. (a) The percentage of ammonium absorbed by various PAA gels at different soaking time. black square) PAA with no treatment, (red circle) PAA treated by water, (blue triangle) PAA treated by phosphate buffer; (b) The percentage of ammonium eluted from various ammonium-absorbed PAA gels soaked in DI water as the function of soaking time. (■) PAA with no treatment, (red circle) PAA treated by water,(blue triangle) PAA treated by phosphate buffer; (c) The percentage of ammonium absorbed by PB treated PAA gels against initial NH_4^+ concentrations; (d) FTIR spectra of freshly prepared x-PAA hydrogel (black), water treated x-PAA upon NH_4^+ absorption (red), and PB treated x-PAA upon NH_4^+ absorption (blue); (e) N 1s peak of freshly prepared x-PAA hydrogel; (f) N 1s peak of PB treated x-PAA upon NH_4^+ absorption.

The UV degradation of PAA also proved to be extremely slow, with a rate constant of only 5.72×10^{-9}.[57] Fall cone test revealed that surficial soil strength remained above 200 kPa under all sample preparation conditions (Table S3). This result indicated that EICP/t-AA treated soils remained strong enough for surficial applications after exposed to heat and UV irradiations. By using kinetic equations and data,[58−62] it was estimated that PAA hydrogels should be stable for at least 3 months even in the extreme weather in Phoenix area,[63] which is sufficiently long for most surficial applications, e.g. dust mitigation at construction sites/mine sites and setting up temporary roads. Detailed calculations are included in the Supporting Information.

Ammonium Mitigation by PAA Hydrogel. Last but importantly, the hydrogel had the ability to mitigate the hazardous byproduct, ammonium, from the EICP process (experimental details are included in the Supporting Information). After adding PAA, the ammonium concentration dropped quickly for the first few (5−10) hours and then leveled out for all the samples (Figure 4a). It was found that the ammonium removal rate could be tuned by pretreating the hydrogel with different agents. Phosphate buffer (PB) treated hydrogel possessed the highest ammonium removal ability and reached an ammonium removal rate of up to 96%. Water treated hydrogel also showed a slightly higher NH_4^+ absorption rate than untreated PAA. After removal from the ammonium solution, all of the hydrogels were rinsed with water to test their ammonium retention ability. PB treated PAA showed only ~3% ammonium release, demonstrating that the fixation of ammonium can be very durable (Figure 4b). The removal of ammonium was efficient even for low NH_4^+ concentrations (Figure 4c). For example, with an initial NH_4^+ concentration of 1 mM, the removal rate reached ~80%, corresponding to only ~200 μM ammonium ions left in the soil.

The absorption of ammonium was verified by FTIR spectra (Figure 4d). The FTIR spectrum of PAA showed an intense C═O stretching band at 1695 cm^{-1}. After soaking in 1 M NH_4^+ solution, water treated PAA showed two peaks at 1400 and 1545 cm^{-1}, corresponding to the symmetric (ν_s) and asymmetric vibration (ν_a) of carboxylate group. Meanwhile, the peak intensity at 1695 cm^{-1} decreased. The ν_a - ν_s value was smaller than that of sodium carboxylate, indicating that bidentate complexes between ammonium and the hydrogel should form.[64,65] Further decreasing in the 1695 cm^{-1} to 1545 cm^{-1} peak ratio was observed for PB treated PAA, indicating a higher degree of deprotonation of carboxyl groups. The result clearly showed that ammonium was absorbed by deprotonated carboxyl groups. A higher ammonium removal efficiency could be reached when carboxyl deprotonation was facilitated, for example, by treating with basic buffers. The weak peak at ~1530 cm^{-1} for freshly prepared PAA was assigned to the N−H bending mode of Bis.[66]

An increase of the atom% of N from 1.53% to 13.89% has been observed by XPS after soaking PB treated PAA hydrogel in ammonium solution. The N 1s emissions for pure PAA hydrogel showed two peaks at 400.5 and 401.8 eV associated with the amide moiety in bis and the trace amount of NH_4^+ from APS (Figure 4e)[67,68] After ammonium absorption, the NH_4^+ peak intensity significantly increased, demonstrating a strong absorption of ammonium at PAA surface (Figure 4f). The measured peak area ratio of N 1s(NH_4^+) to N 1s(amide) equaled to 13.7, close to one-half of the molar ratio of carboxyl to amide groups in the hydrogel (21.5). This supported our previous conclusion that NH_4^+ majorly formed bidentate

DOI: 10.1021/acs.est.6b01285
Environ. Sci. Technol. 2016, 50, 12401−12410

complex with PAA. Due to the chelating structure, NH_4^+-PAA complex is relatively stable and therefore can withstand water rinses. A higher removal rate was seen with increasing initial NH_4^+ concentrations (Figure 4c), probably because the chelation of ammonium helped to bring polymer chains closer, favoring further binding events.

This work demonstrated a novel synthetic method to prepare PAA-based biomimetic hydrogel structures for soil stabilization. It was shown that by in situ polymerization, a PAA hydrogel spontaneously grew into a hierarchical dendritic network that not only bore a high similarity to a plant root structure but also mimicked several soil stabilization functions of root systems through effectively binding sand into a remarkably strong cohesive soil crust, achieving the water retention, ion absorption, and soil aggregation capabilities in a chemically controllable manner. Although previous polymer based soil stabilizers can reach similar level of water retention ability and thermal stabilities, none of them has demonstrated such a versatility in functions that our method shows.[69,70] An additional benefit of jointly using EICP and hydrogel was enhancing the mechanical strength of hydrogel through the complexation of hydrogel with the cations in the complex system. As a result, this approach significantly enhanced soil strength, with the as-obtained soil crust sustaining a pressure as high as 4.8×10^3 kPa. The hydrogel and EICP worked synergistically to provide a versatile, high-performance soil stabilization method. SEM images showed that a polymer/calcite composite was formed, in which the calcite crystals grew and were well dispersed in the porous hydrogel network to tightly bind the soil grains together. Compared with conventional EICP, the addition of PAA was able to retain water for a longer biomineralization time and localize the mineralization at the soil surface. The application of PAA also helped to remove the unwanted NH_4^+ byproduct from reaction system. Spectral data showed that ammonium ions were effectively absorbed by carboxyl groups in the PAA, leading to a reduced concentration of ammonium in the reaction system. The absorption of ammonium was relatively stable and could sustain moderate rinsing with water.

While hydrogels and EICP can be applied individually for soil stabilization, their combination appears to significantly improve the adaptability and versatility of both techniques for soil stabilization. For instance, by simply varying their relative ratios, the stiffness, thickness and chemical properties of a surficial soil crust might be tuned over a wide range. A high EICP-to-hydrogel ratio would be more suitable for temporal soil fixation (e.g., fugitive dust control on a construction site) as it could be removed easily. On the other hand, a hydrogel-dominant recipe may be used in permanent, heavy duty tasks, including surface water erosion control (e.g., channel linings) and improving low volume road surfaces. By varying the functional groups in the hydrogel, it is also possible to realize other contaminant mitigation functions during soil stabilization, including but not limit to removing Pb, Hg and Cr ions. We believe this highly versatile and sustainable method can also find broad applications in tunneling, foundation bearing capacity enhancement, and soil liquefaction mitigation.

■ ASSOCIATED CONTENT

Supporting Information

The Supporting Information is available free of charge on the ACS Publications website at DOI: 10.1021/acs.est.6b01285.

Detailed experimental procedure, additional results and discussions regarding sample characterization, mechanical test, water retention and accelerated weathering test. A video demonstrating the hardness of the EICP/t-AA treated soil sample (PDF)
(MPG)

■ AUTHOR INFORMATION

Corresponding Author

*Phone: +1-4807272944; e-mail: Ximin.He@asu.edu.

Notes

The authors declare no competing financial interest.

■ ACKNOWLEDGMENTS

This work was supported by the National Science Foundation under grant EEC-1449501 and grant CMMI-1233658. The authors are grateful for the NSF support. Any opinions or positions expressed in this paper are the opinions and positions of the authors only, and do not reflect any opinions or positions of the NSF.

■ REFERENCES

(1) Stern, D. I.; Common, M. S.; Barbier, E. B. Economic growth and environmental degradation: the environmental kuznets curve and sustainable development. *World Development* **1996**, *24* (7), 1151−1160.
(2) *Air Pollution Engineering Manual*, 2nd, ed.; Davis, W. T., Ed.; John Wiley & Sons: New York, 2000.
(3) Fernando, H. J.; Mammarella, M. C.; Grandoni, G.; Fedele, P.; Di Marco, R.; Dimitrova, R.; Hyde, P. Forecasting PM10 in metropolitan areas: efficacy of neural networks. *Environ. Pollut.* **2012**, *163*, 62−67.
(4) Zobeck, T. M. Soil properties affecting wind erosion. *Journal of Soil and Water Conservation* **1991**, *46* (2), 112−118.
(5) Borja, R. I. Condition for liquefaction instability in fluid-saturated granular soils. *Acta Geotechnica* **2006**, *1* (4), 211−224.
(6) Kezdi, A.; Rethati, L. *Handbook of Soil Mechanics: Soil Mechanics of Earthworks Foundations and Highway Engineering*; Elsevier's Science and Technology: Oxford, U.K., 1988.
(7) Cheng, X.; Zheng, G.; Soga, K.; Bandara, S. S.; Kumar, K.; Diao, Y.; Xu, J. Post-failure behavior of tunnel heading collapse by MPM simulation. *Sci. China: Technol. Sci.* **2015**, *58* (12), 2139−2152.
(8) Sarioglu, M. Removal of ammonium from municipal wastewater using natural Turkish (Dogantepe) zeolite. *Sep. Purif. Technol.* **2005**, *41* (1), 1−11.
(9) Li, X. Z.; Zhao, Q. L.; Hao, X. D. Ammonium removal from landfill leachate by chemical precipitation. *Waste Manage.* **1999**, *19* (6), 409−415.
(10) Schultz, B.; Kjeldsen, P. Screening of organic matter in leachates from sanitary landfills using gas chromatography combined with mass spectrometry. *Water Res.* **1986**, *20* (8), 965−970.
(11) Guo, L. Doing battle with the green monster of Taihu Lake. *Science* **2007**, *317* (5842), 1166.
(12) Zheng, Y.; Wang, A. Preparation and ammonium adsorption properties of biotite-based hydrogel composites. *Ind. Eng. Chem. Res.* **2010**, *49* (13), 6034−6041.
(13) Avrahami, S.; Conrad, R.; Braker, G. Effect of Soil Ammonium concentration on N2O release and on the community structure of ammonia oxidizers and denitrifiers. *Appl. Environ. Microbiol.* **2002**, *68* (11), 5685−5692.
(14) King, G. M.; Schnell, S. Effect of increasing atmospheric methane concentration on ammnium inhibition of soil methane consumption. *Nature* **1994**, *370* (6487), 282−284.
(15) Prusinski, J.; Bhattacharja, S. Effectiveness of Portland cement and lime in stabilizing clay soils. *Transp. Res. Rec.* **1999**, *1652*, 215−227.

(16) Mehta, P. K. Reducing the environmental impact of concrete. *Concrete international* **2001**, *23* (10), 61−66.
(17) *Surface-aggregate stabilization with chloride materials*; 0677−1805-SDTDC; U.S. Department of Agriculture, Forest Service, National Technology and Development Program: Washington, DC, 2006; www.fs.fed.us/t-d/pubs/pdf/06771805.pdf.
(18) Galán-Marín, C.; Rivera-Gómez, C.; Petric, J. Clay-based composite stabilized with natural polymer and fibre. *Construction and Building Materials* **2010**, *24* (8), 1462−1468.
(19) Orts, W. J.; Roa-Espinosa, A.; Sojka, R. E.; Glenn, G. M.; Imam, S. H.; Erlacher, K.; Pedersen, J. S. Use of synthetic polymers and biopolymers for soil stabilization in agricultural, construction, and military applications. *J. Mater. Civ. Eng.* **2007**, *19* (1), 58−66.
(20) Liu, J.; Shi, B.; Jiang, H.; Huang, H.; Wang, G.; Kamai, T. Research on the stabilization treatment of clay slope topsoil by organic polymer soil stabilizer. *Eng. Geol.* **2011**, *117* (1), 114−120.
(21) Gross, R. A.; Kalra, B. Biodegradable polymers for the environment. *Science* **2002**, *297* (5582), 803−807.
(22) Lambers, H. Dryland salinity: a key environmental issue in southern Australia. *Plant Soil* **2003**, *257* (2), v−vii.
(23) Woolard, C. R.; Irvine, R. L. Treatment of hypersaline wastewater in the sequencing batch reactor. *Water Res.* **1995**, *29* (4), 1159−1168.
(24) Karraker, N. E.; Gibbs, J. P.; Vonesh, J. R. Impacts of road deicing salt on the demography of vernal pool-breeding amphibians. *Ecological Applications* **2008**, *18* (3), 724−734.
(25) Holten-Andersen, N.; Jaishankar, A.; Harrington, M.; Fullenkamp, D. E.; DiMarco, G.; He, L.; McKinley, G. H.; Messersmith, P. B.; Lee, K. Y. Metal-coordination: using one of nature's tricks to control soft material mechanics. *J. Mater. Chem. B* **2014**, *2* (17), 2467−2472.
(26) Rae Cho, K.; Kim, Y. Y.; Yang, P.; Cai, W.; Pan, H.; Kulak, A. N.; Lau, J. L.; Kulshreshtha, P.; Armes, S. P.; Meldrum, F. C.; De Yoreo, J. J. Direct observation of mineral-organic composite formation reveals occlusion mechanism. *Nat. Commun.* **2016**, *7*, 10187.
(27) Neupane, D.; Yasuhara, H.; Kinoshita, N.; Unno, T. Applicability of enzymatic calcium carbonate precipitation as a soil-strengthening technique. *J. Geotech. Geoenviron. Eng.* **2013**, *139* (12), 2201−2211.
(28) Neupane, D.; Yasuhara, H.; Kinoshita, N. Soil Improvement through enzymatic calcite precipitation technique: small to large scale experiments. *Int. J. Lsld. Env.* **2013**, *1* (1), 65−66.
(29) Yasuhara, H.; Neupane, D.; Hayashi, K.; Okamura, M. Experiments and predictions of physical properties of sand cemented by enzymatically-induced carbonate precipitation. *Soils and Foundations* **2012**, *52* (3), 539−549.
(30) van Oss, H. G.; Padovani, A. C. Cement manufacture and the environment part I: chemistry and technology. *J. Ind. Ecol.* **2002**, *6* (1), 89−105.
(31) van Oss, H. G.; Padovani, A. C. Cement manufacture and the environment part II: environmental challenges and opportunities. *J. Ind. Ecol.* **2003**, *7* (1), 93.
(32) DeJong, J. T.; Fritzges, M. B.; Nüsslein, K. Microbially induced cementation to control sand response to undrained shear. *J. Geotech. Geoenviron. Eng.* **2006**, *132* (11), 1381−1392.
(33) Maghchiche, A.; Haouam, A.; Immirzi, B. Use of polymers and biopolymers for water retaining and soil stabilization in arid and semiarid regions. *Journal of Taibah University for Science* **2010**, *4*, 9−16.
(34) Demitri, C.; Scalera, F.; Madaghiele, M.; Sannino, A.; Maffezzoli, A. Potential of cellulose-based superabsorbent hydrogels as water reservoir in agriculture. *Int. J. Polym. Sci.* **2013**, *2013*, 435073.
(35) Kim, P.; Zarzar, L. D.; He, X.; Grinthal, A. Aizenberg, Hydrogel-actuated integrated responsive systems (HAIRS): Moving towards adaptive materials. *Curr. Opin. Solid State Mater. Sci.* **2011**, *15* (6), 236−245.
(36) He, X.; Aizenberg, M.; Kuksenok, O.; Zarzar, L. D.; Shastri, A.; Balazs, A. C.; Aizenberg, J. Synthetic homeostatic materials with chemo-mechano-chemical self-regulation. *Nature* **2012**, *487* (7406), 214−218.
(37) Shastri, A.; McGregor, L. M.; Liu, Y.; Harris, V.; Nan, H.; Mujica, M.; Vasquez, Y.; Bhattacharya, A.; Ma, Y.; Aizenberg, M.; Kuksenok, O.; Balazs, A. C.; Aizenberg, J.; He, X. An aptamer-functionalized chemomechanically modulated biomolecule catch-and-release system. *Nat. Chem.* **2015**, *7* (5), 447−454.
(38) Hamdan, N.; Zhao, Z.; Kavazanjian, E., Jr.; He, X. Hydrogel-assisted Enzyme Induced Carbonate Mineral Precipitation. *J. Mater. Civ. Eng.* **2016**, *28*, 04016089.
(39) Garrigues, E.; Doussan, C.; Pierret, A. Water Uptake by Plant Roots: I - Formation and propagation of a water extraction front in mature root systems as evidenced by 2D light transmission imaging. *Plant Soil* **2006**, *283* (1−2), 83−98.
(40) Angers, D. A.; et al. Plant-induced changes in soil structure: processes and feedbacks. In *Plant-Induced Soil Changes: Processes and Feedbacks*; van Breemen, N., Ed.; Springer: Berlin, Germany, 1998; pp 55.
(41) Oades, J. M.; Waters, A. G. Aggregate hierarchy in soils. *Aust. J. Soil Res.* **1991**, *29* (6), 815−828.
(42) Doussan, C.; Pierret, A.; Garrigues, E.; Pagès, L. Water Uptake by Plant Roots: II − Modelling of water transfer in the soil root-system with explicit account of flow within the root system comparison with experiments. *Plant Soil* **2006**, *283* (1−2), 99−117.
(43) Kherb, J.; Flores, S. C.; Cremer, P. S. Role of carboxylate side chains in the cation Hofmeister series. *J. Phys. Chem. B* **2012**, *116* (25), 7389−7397.
(44) Zheng, Y.; Wang, A. Evaluation of ammonium removal using a chitosan-g-poly (acrylic acid)/rectorite hydrogel composite. *J. Hazard. Mater.* **2009**, *171* (1−3), 671−677.
(45) Van Humbeck, J. F.; McDonald, T. M.; Jing, X.; Wiers, B. M.; Zhu, G.; Long, J. R. Ammonia capture in porous organic polymers densely functionalized with Bronsted acid groups. *J. Am. Chem. Soc.* **2014**, *136* (6), 2432−2440.
(46) *Environmental Health Criteria 191: Acrylic Acid*; World Health Organization: Geneva, Switzerland, 1997; www.inchem.org/documents/ehc/ehc/ehc191.htm.
(47) Chen, C. Y.; Chiang, C. L.; Chen, C. R. Removal of heavy metal ions by a chelating resin containing glycine as chelating groups. *Sep. Purif. Technol.* **2007**, *54* (3), 396−403.
(48) Hamdan, N.; Kavazanjian, E., Jr. Enzyme Induced Carbonate Mineral Precipitation for Fugitive Dust Control. *Geotechnique* **2016**, *66* (7), 546−555.
(49) Eliassi, A.; Modarress, H.; Mansoori, G. A. Measurement of activity of water in aqueous poly(ethylene glycol) solutions (effect of excess volume on the Flory-Huggins ø-parameter). *J. Chem. Eng. Data* **1999**, *44* (1), 52−55.
(50) Bercea, M.; Nichifor, M.; Eckelt, J.; Wolf, B. A. Dextran-based polycations: thermodynamic interaction with water as compared with unsubstituted dextran, 2 - Flory/Huggins interaction parameter. *Macromol. Chem. Phys.* **2011**, *212* (17), 1932−1940.
(51) Emerson, J. A.; Toolan, D. T. W.; Howse, J. R.; Furst, E. M.; Epps, T. H. Determination of solvent−polymer and polymer−polymer Flory−Huggins interaction parameters for poly(3-hexylthiophene) via solvent vapor swelling. *Macromolecules* **2013**, *46* (16), 6533−6540.
(52) Wu, Y.; Joseph, S.; Aluru, N. R. Effect of cross-linking on the diffusion of water, ions, and small molecules in hydrogels. *J. Phys. Chem. B* **2009**, *113* (11), 3512.
(53) Fu, Y.; Elsenbaumer, R. L. Thermochemistry and kinetics of chemical polymerization of aniline determined by solution calorimetry. *Chem. Mater.* **1994**, *6* (5), 671−677.
(54) Tanaka, H.; Hirabayashi, H.; Matsuoka, T.; Kaneko, H. Use of fall cone test as measurement of shear strength for soft clay materials. *Soils and Foundations* **2012**, *52* (4), 590−599.
(55) Gopferich, A. Mechanism of polymer degradation and elimination. In *Handbook of Biodegradable Polymers*; Wiseman, D. M., Kost, J., Domb, A. J., Eds.; CRC press: Boca Raton, 1997; pp 451.
(56) Fyfe, C. A.; McKinnon, M. S. Investigation of the thermal degradation of poly (acrylic acid) and poly (methacrylic acid) by high-resolution carbon-13 CP/MAS NMR spectroscopy. *Macromolecules* **1986**, *19* (7), 1909−1912.

DOI: 10.1021/acs.est.6b01285
Environ. Sci. Technol. 2016, 50, 12401−12410

(57) Aarthi, T.; Shaama, M. S.; Madras, G. Degradation of water soluble polymers under combined ultrasonic and ultraviolet radiation. *Ind. Eng. Chem. Res.* **2007**, *46* (19), 6204−6210.
(58) Laidler, K. J. The development of the Arrhenius equation. *J. Chem. Educ.* **1984**, *61* (6), 494.
(59) Greenberg, A. R.; Kamel, I. Kinetics of anhydride formation in poly (acrylic acid) and its effect on the properties of a PAA-alumina composite. *J. Polym. Sci., Polym. Chem. Ed.* **1977**, *15* (9), 2137−2149.
(60) Wall, L. A.; Flynn, J. H. Degradation of polymers. *Rubber Chem. Technol.* **1962**, *35* (5), 1157−1221.
(61) Rabek, J. F. *Polymer photodegradation: mechanisms and experimental methods*; Springer: Berlin, Germany, 1995.
(62) Koerner, R. *Geotextiles: From Design to Applications*; Woodhead Publishing: Sawston, U.K., 2016.
(63) U. S. climate data − Phoenix. http://www.usclimatedata.com/climate/phoenix/arizona/united-states/usaz0166.
(64) Deacon, G. B.; Phillips, R. J. Relationships between the carbon-oxygen stretching frequencies of carboxylato complexes and the type of carboxylate coordination. *Coord. Chem. Rev.* **1980**, *33* (3), 227−250.
(65) Tang, F.; Huang, X.; Wang, L.; Guo, J. Infrared spectral studies of ammonium polyacrylate adsorbed on nano-zirconia powder surfaces. *Nanostruct. Mater.* **1999**, *11* (7), 861−866.
(66) Reddy, B. V.; Rao, G. R. Vibrational spectra and modified valence force field for N, N′-methylenebisacrylamide. *Indian Journal of Pure & Applied Physics* **2008**, *46*, 611−616.
(67) Moulder, J. F. *Handbook of X-ray Photoelectron Spectroscopy: A Reference Book of Standard Spectra for Identification and Interpretation of XPS Data*; Perkin-Elmer Corporation, Physical Electronics Division: Eden Prairie, 1995.
(68) Solomun, T.; Schimanski, A.; Sturm, H.; Illenberger, E. Reactions of amide group with fluorine as revealed with surface analytics. *Chem. Phys. Lett.* **2004**, *387* (4), 312−316.
(69) Lee, S. S.; Chang, S. X.; Chang, Y. Y.; Ok, Y. S. Commercial versus synthesized polymers for soil erosion control and growth of Chinese cabbage. *SpringerPlus* **2013**, *2* (1), 1.
(70) Maghchiche, A.; Haouam, A.; Immirzi, B. Use of polymers and biopolymers for water retaining and soil stabilization in arid and semiarid regions. *Journal of Taibah University for Science* **2010**, *4*, 9−16.

DOI: 10.1021/acs.est.6b01285
Environ. Sci. Technol. 2016, 50, 12401−12410